# Electronic properties of the leaky quantum-well system Ag(111)/Au/Ag

W. E. McMahon,* T. Miller, and T.-C. Chiang
*Department of Physics, University of Illinois at Urbana-Champaign, 1110 West Green Street, Urbana, Illinois 61801-3080 and Seitz Materials Research Laboratory, University of Illinois at Urbana-Champaign, 104 South Goodwin Avenue, Urbana, Illinois 61801-2902*

(Received 7 March 1996; revised manuscript received 8 May 1996)

Angle-resolved photoemission has been employed to examine the electronic properties of a lattice-matched, epitaxial system prepared by depositing first a thin Au(111) layer on a Ag(111) substrate, and then a Ag(111) overlayer. The Au layer acts as a potential barrier for electron motion in the system. The Ag overlayer can be regarded as a quantum well, but in our experiment, the Au barrier is rather thin, and there is substantial coupling between the valence electrons in the Ag overlayer and the continuum states in the substrate. Nevertheless, well-defined quantum-well resonances are observed for Au barriers as thin as two atomic layers. These resonances can be understood as a result of partial trapping of valence electrons in the Ag overlayer. A calculation which takes into account the band structure and surface properties is carried out, and the results are in good agreement with the experiment. Initial- and final-state features in the spectra are identified by comparison with theoretical models. The effects of lattice match or mismatch at the interface will be discussed. [S0163-1829(96)02439-3]

## I. INTRODUCTION

Metallic layered systems have attracted much interest in recent years. Quantum-mechanical effects associated with small dimensions such as electron confinement have been observed, suggesting possible applications as quantum devices.[1–16] A well-known example is the giant magnetoresistance effect, which is potentially important for the magnetic recording industry.[10–13] Spin valves and spin transistors are other possibilities.[10] Although it is generally recognized that quantum-mechanical effects play an important role in determining the electronic and electrical properties of such systems, the state of our knowledge is far from complete. When layered systems are actually made in a laboratory, there are materials issues that require attention, including lattice match/mismatch, defects, and band-structure effects. All of these problems need to be considered and understood in a quest for technological advances.

The purpose of this paper is to examine some of the basic issues related to the quantum-mechanical behaviors of layered structures. To separate out issues related to structural and electronic effects, the system under study is chosen to have a very simple configuration. We begin with a Ag(111) substrate, and then deposit a layer of Au to form a barrier layer. On top of the Au barrier, we then deposit a slab of Ag to form a ''quantum well.'' Due to band misalignment between Ag and Au, the electrons in the Ag slab with energies above the Au band edge along the [111] direction would be confined if the Au were sufficiently thick (quantum-well limit).[5] In our experiment, we purposely made the Au barrier thin, so there is significant coupling between the valence electrons in the Ag slab and the substrate continuum states. The resulting system can be described as a leaky quantum well, and all of the Ag valence states, except for the surface states, extend throughout the entire system. One reason for our interest in such a system stems from a desire to understand the general behavior of an overlayer on a substrate. Most such bimetallic overlayer systems do not have band gaps for electron confinement, but the band misalignment can cause partial electron reflection at an interface, which is the origin for many of the quantum-mechanical effects observed in metallic layered systems. The Au barrier in our Ag/Au/Ag samples also causes partial reflection. Experimentation with Ag/Au/Ag is, however, a better way to understand such interface coupling effects, because the barrier thickness can be experimentally varied to change this coupling strength. Another advantage is that the slab and the substrate in the present case are both Ag, and have the same band structure, making a theoretical calculation a much simpler task than for a general bimetallic system involving different band structures. Yet one more advantage is that Ag and Au are lattice matched, again leading to considerable simplification in the theoretical treatment.

Our experiment is an angle-resolved photoemission measurement of the electronic excitation spectra for the Ag/Au/Ag system. Angle-resolved photoemission is perhaps the most direct probe of the electronic properties, and has been widely employed for band-structure determination. However, this probe involves both an initial state and a final state which are linked by the photoexcitation process. A proper understanding of the experimental results must consider both the initial and the final states. For the system under study, the states involved are highly delocalized valence and conduction states, and consequently, many-body effects associated with the dynamic response of the system such as electronic relaxation and hole screening can be ignored. This simplification permits us to use a single-particle model involving Bloch states and the band structure to compute the photoemission spectra and various other quantities. The results of this calculation are compared with the experiment, and a detailed analysis allows us to draw some conclusions about the wave functions and to assign features in the spectra to effects pertaining to the initial states or the final states.

The main results are (1) well-defined quantum-well reso-

 

nances (QWR's) in the Ag slab are observed for Au barriers as thin as two atomic layers, (2) these QWR's are dominated by initial-state effects and do not show energy dispersions as the excitation photon energy is varied, and (3) final-state effects for these QWR's are generally small, but become important near the band-to-band transitions. Conclusion (2) might be surprising at first sight, because a previous study of a bimetallic system, Ag on Ni(111), has shown QWR features that exhibit ratcheting energy dispersions and oscillatory intensity modulations as the excitation photon energy is varied.[17] Furthermore, it has been shown that both the initial and final states are generally important for that system. Since electron coupling at an interface is the same underlying mechanism for the phenomena observed in Ni(111)/Ag and Ag(111)/Au/Ag, a question arises as to why these two systems exhibit very different behaviors. The difference, as we will discuss in detail, is mainly caused by the lattice mismatch for the Ni(111)/Ag system. Thus, lattice match/mismatch is an important factor in governing the overall behaviors of QWR's.

## II. EXPERIMENTAL DETAILS

The Ag(111) substrate used in our experiment was cut from a single-crystal ingot, oriented by x-ray Laue diffraction, and mechanically polished to a mirror finish. The sample was then electropolished, and transferred into a vacuum chamber. Surface preparation was done by repeated sputtering with low-energy argon ions and annealing. The final surface showed no signs of contamination by photoemission or Auger, and exhibited a sharp $(1\times1)$ electron-diffraction pattern. Photoemission from the same surface showed an intense surface state, suggesting a well ordered and flat surface. Independent scanning tunneling microscopy studies of similarly prepared samples showed large atomically flat terraces separated by atomic steps.

Au and Ag deposition on the substrate was done by thermal evaporation from tungsten crucibles containing high-purity materials. The crucibles were heated by an electron beam, which was feedback controlled. The deposition rate was monitored by a water-cooled quartz oscillator. The sample was kept at room temperature during deposition. Previous studies of samples prepared under the same conditions indicated that the resulting Ag-Au interfaces were fairly abrupt.[18] The sample surface after growth was checked with electron diffraction, which revealed a sharp $(1\times1)$ pattern.

The photoemission measurements were performed at the Synchrotron Radiation Center, University of Wisconsin, Stoughton, Wisconsin. A small hemispherical analyzer with a 3° full acceptance cone was used to collect the data. All spectra reported in this work were taken with a normal-emission geometry. The system resolution was typically set at ~0.1 eV or better. The sample was kept at room temperature during the measurements.

## III. EXPERIMENTAL RESULTS

A large data set was collected for various sample configurations and photon energies. Figures 1–3 show a subset which illustrates the main results of this study. The left panel of Fig. 1 is a stack plot of spectra for various photon energies

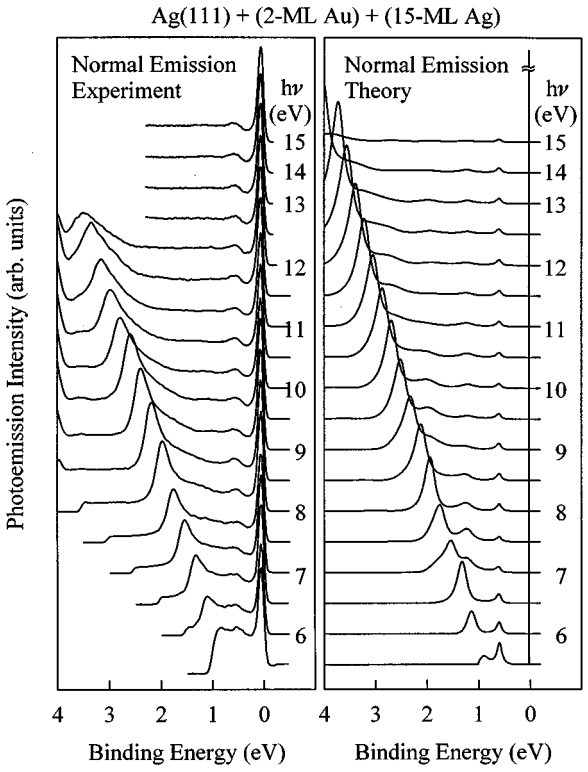


FIG. 1. Experimental (left) and theoretical (right) normal-emission spectra for Ag(111)+(2-ML Au)+(15-ML Ag). The photon energies are indicated; the unlabeled spectra are taken at 0.5-eV intervals. The binding energy is referred to the Fermi level.

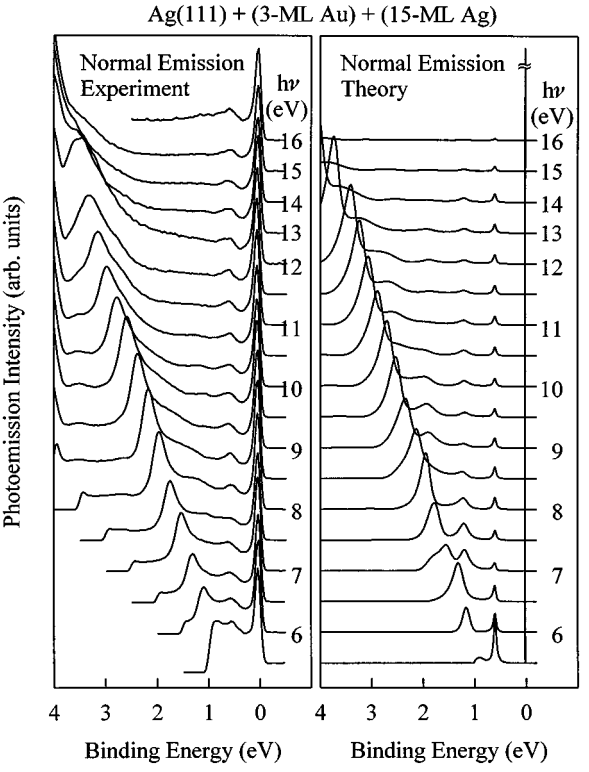


FIG. 2. Same as Fig. 1, except that the Au barrier thickness is 3 ML.

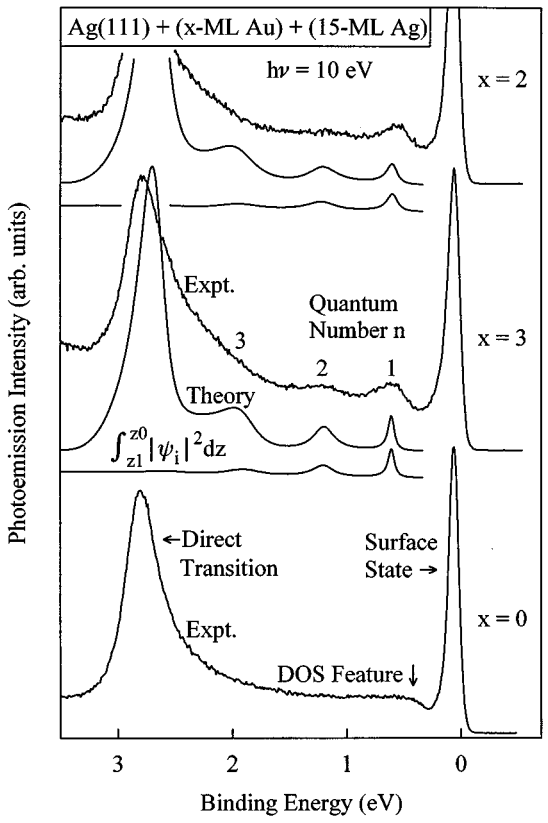


FIG. 3. Experimental and theoretical normal-emission spectra for the two samples ($x=2$ and 3) taken with a photon energy of 10 eV. Curves corresponding to the initial-state probability in the Ag slab are also shown for comparison. The bottom curve is an experimental spectrum taken from pure Ag(111) ($x=0$).

as indicated in the figure. The sample configuration was a 15-ML Ag slab on top of a 2-ML Au barrier. The right panel of the same figure is the corresponding spectra from a calculation to be described below. Figure 2, constructed in the same way as Fig. 1, summarizes the results for a similar sample with a thicker barrier of 3-ML Au. These two figures provide an overview of the behavior of various spectral features, some of which may be too small for a detailed viewing, however. To facilitate a detailed comparison, Fig. 3 shows a magnified spectrum for each of the two systems, taken with a photon energy of 10 eV. The magnified theoretical spectra are shown for comparison. This figure also includes calculated initial-state probability curves, which will be discussed later. The bottom spectrum in Fig. 3 is taken from pure Ag(111) at the same photon energy for comparison. For simplicity, we use $x$ to denote the thickness of the barrier in ML, so $x=2$ and 3 for the two sample configurations shown, and $x=0$ for pure Ag(111). In these figures, the narrow intense peak just below the Fermi level is derived from a Shockley surface state of Ag(111).[5,19–22] The experimental spectra are normalized to this peak intensity.

## IV. MODEL CALCULATION

Since our normal-emission geometry detects electrons traveling perpendicular to the surface, we need to consider the band structure along the [111] direction only. The problem becomes effectively one dimensional. The band structures of Ag and Au are very similar. There is a free-electron-like $sp$ band and five $d$ bands in the valence-band region. The top of the Ag $d$ bands is at about 4 eV below the Fermi level. In our study, we will focus our attention on the portion of the free-electron-like $sp$ band above the $d$ bands. For photon energies less than ~50 eV, the final band for photoexcitation is the same $sp$ band folded back once into the first Brillouin zone by the crystal potential. A basis consisting of two plane waves $\exp(ikz)$ and $\exp[i(k-g)z]$ thus provides a fairly good description for the initial- and final-band dispersions, where $g=2.66$ Å$^{-1}$ is the first reciprocal-lattice vector along the [111] direction. This is the well known two band model.[22] To account for hybridization to other bands to first order, we employ an effective electron mass, which is chosen to yield a good fit to the dispersion of the $sp$ band near the Fermi level.[22,23] This fit works well near the Fermi level, but deviates as the binding energy increases toward the top of the $d$ bands beginning at 4 eV. The Au band structure can be described fairly well by simply shifting the Ag band structure downward to higher binding energies by 0.77 eV.

In our calculation, the wave functions in Ag and Au are constructed using analytic forms of the Bloch states. In general, each wave function is a linear combination of two Bloch states at the same energy, one traveling toward $+z$, and the other toward $-z$, for a total of four plane-wave states. The interface between Ag and Au is modeled by an abrupt boundary, where the wave functions are matched analytically. For the Ag-vacuum interface, we assume a step potential determined by the work function of Ag. The position of this potential step, at $z=z0$, does not necessarily coincide with the classical surface due to electrons spilling over into the vacuum side. A separate calculation is performed for a semi-infinite Ag(111) substrate, and the binding energy of the Shockley surface state as a function of $z0$ is computed. By setting this binding energy to the experimentally observed value, $z0$ is uniquely determined. This assures us that the wave functions on the two sides of the vacuum boundary have the correct relative phases at the energy of the surface state. Since the energy range of interest is fairly small, the errors at other energies will be small. The wave function in the vacuum is just an exponentially decaying wave in the initial state, and a linear combination of plane-wave states in the final state. These waves are matched to the linear combination of Bloch states in the Ag slab.

For the photoemission process, the final state is one in which an electron is captured by the detector. It is much easier conceptually to consider the time-reversed state, in which an electron is sent from the detector to the sample. The result is similar to a low-energy-electron-diffraction (LEED) experiment,[24] where the incident electron is partially transmitted and partially reflected. The transmitted electron in the solid is attenuated by inelastic scattering, which is modeled in our case by using an exponentially decaying envelope function. The mean free path $L$ is usually defined in terms of the electron current, and so $2L$ is used to describe the wave-function amplitude decay. Reversing this LEED wave function in time yields our final state for photoemission. Including the mean free path in the calculation is important; without it, the matrix element integral is mathematically ill defined. For the calculated spectra shown in Figs.

1–3, we assume a constant mean free path of $L=20$ Å. The mean free path does depend on the photoelectron kinetic energy, but this variation is small and unimportant for the present discussion as verified by separate calculations.[25]

The momentum matrix element is calculated using the above described wave functions. The photoemission spectra are computed using Fermi's golden rule, and the initial and final density of states are included. Since it is difficult to measure absolute photoemission intensities, we have normalized the spectra to the photoemission intensity of the Shockley surface state, which is also calculated. These normalized theoretical spectra are shown in Figs. 1 and 2. The surface state is an eigenstate of the system, and has the shape of a $\delta$ function. It is schematically indicated in Figs. 1 and 2 by a spike just below the Fermi level.

Our ''one-step'' calculation[26] thus involves both the band structure and surface properties. Inelastic scattering in the final state is included. Since the mean free path for this inelastic scattering is much shorter than the coherence length of the initial state, the latter is ignored (assumed to be $\infty$). One effect that is not included in our calculation is the hole lifetime broadening, because we do not have detailed data for this broadening. This broadening is on the order of a fraction of an eV, becoming larger at higher binding energies. The wave functions derived from our calculations should be understood as pseudo wave functions. They represent the real wave functions well in the interstitial region, but not necessarily in the core region. This approximation does not affect the wave-function matching, which occurs in the interstitial region, and has only a small effect on the matrix element, because the core region has a very small volume.

## V. DISCUSSION

### A. Ag(111)-like features

An inspection of Figs. 1–3 reveals that the overall features of the experimental data are well reproduced by the calculation. The two most intense features in the spectra are the Shockley surface-state peak just below the Fermi level and the so-called direct-transition peak (see Fig. 3), which moves as the photon energy changes. Both features appear very similar to those seen in pure Ag(111),[19–21] which is to be expected. Since the top 15 atomic layers are Ag for our Ag/Au/Ag sample, the surface state should be Ag(111)-like. The direct-transition peak is derived from a vertical band-to-band transition in the bulk involving the $sp$ wave function over many atomic planes (limited by the mean free path), which should be fairly insensitive to the 2 or 3 ML of Au inserted into the lattice. With a photon energy of $h\nu=5.5$ eV, the direct-transition peak is at about a 1-eV binding energy, which happens to be very close to the vacuum cutoff defined by the work function of 4.49 eV for Ag(111). As a result, the direct-transition peak nearly disappears, and the experimental spectra are dominated by an inelastic background. As the photon energy increases, the direct-transition peak moves to higher binding energies. Relative to the theory, one can see that this peak becomes broader and weaker at higher photon energies as it moves close to the $d$-band threshold at around a 4-eV binding energy (the $d$-band threshold is seen as a sharp upturn in the experimental spectra at the left edge of Figs. 1 and 2). This gradual deviation from theory is due to an increased mixing of the $d$ character into the initial $sp$ state as the binding energy increases. Close to the Shockley surface state, there is a subtle feature for the pure Ag(111) case as seen in Fig. 3, which is labeled a density-of-states (DOS) feature. This has been observed before and can be attributed to ''indirect transitions'' from the $sp$ valence band which has a band edge at 0.33 eV.[19,20]

### B. Quantum-well resonances

In addition to the Ag(111)-like features mentioned above, several weak peaks are present in the Ag/Au/Ag spectra, which have no counterparts in pure Ag. These are QWR's associated with the layered structure and are labeled in Fig. 3 by the ''quantum numbers'' $n=1-3$. These correspond to electrons partially trapped in the Ag slab caused by the Au barrier potential, and become better defined as the barrier thickness increases. The Au $sp$ band edge is at about 1.1 eV binding energy. If the Au barrier were infinitely thick, one would expect the $n=1$ state to be a true quantum-well state, because its energy would be in the Au band gap. In our case, the Au barrier is very thin, and there is no confinement. Nevertheless, well-defined QWR's are observed. An important observation here is that the QWR's have fixed binding energies, independent of the excitation photon energy.

The experimental QWR peaks are much broader than the theoretical ones. This broadening is more severe for larger quantum numbers at higher binding energies. Figure 3 shows that the $n=3$ QWR is broadened to almost beyond recognition, becoming an asymmetric tail of the direct-transition peak. Its contribution to the photoemission intensity can be seen as an increased emission in the tail region by comparing the Ag/Au/Ag spectra to the corresponding pure Ag(111) spectrum shown in Fig. 3. A careful inspection of Figs. 1 and 2 also reveals the presence of this subtle feature. This increase in broadening in going to higher binding energies is consistent with the general trend of the hole lifetime, but the magnitude of the broadening observed here appears too large. The hole lifetime can be estimated from the line shape of the direct transition, and should be much less than 0.5 eV. Sample imperfection provides a plausible explanation for the severe broadening of the $n=3$ QWR. We will return to this point after we have examined the wave functions.

### C. Initial wave functions

The $n=1$ and 2 QWR's are at binding energies of 0.60 and 1.23 eV, respectively. Figure 4 shows some calculated initial-state wave functions at these and other energies. In this figure, $z=0$ is at the classical surface, and the vertical dashed lines indicate the various boundaries between Ag, Au, and vacuum. The wave functions appear as short-period oscillations superimposed on an envelope function oscillating at a longer period. The short oscillation period is roughly twice the atomic layer spacing in the [111] direction, because the Bloch states have a wave vector very close to the Brillouin-zone boundary. The long period is determined by how far away this wave vector is from the Brillouin-zone boundary. Basically, it is the period of beating between the plane waves making up the Bloch state. The farther away

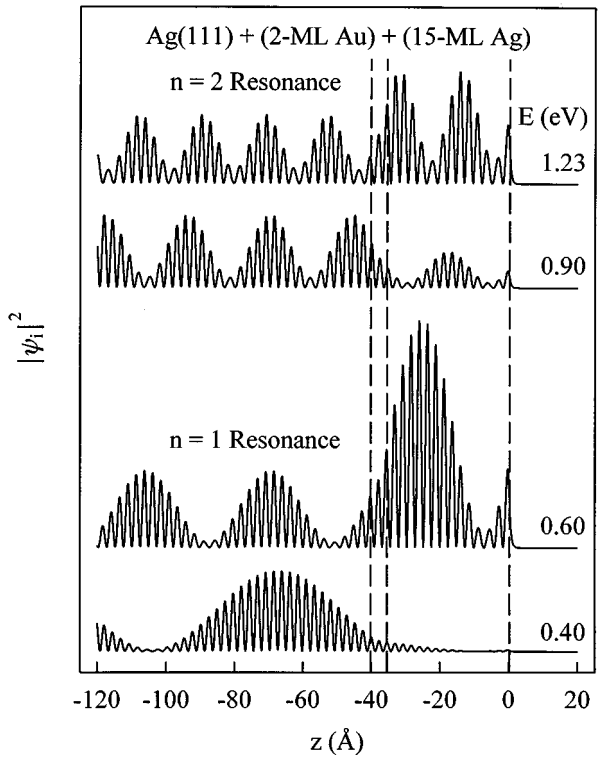


FIG. 4. The absolute square of the initial wave function at several binding energies as indicated. The origin of the $z$ axis is at the classical surface plane. The vertical dashed lines indicate the various boundaries between Ag, Au, and vacuum for the sample with $x=2$.

from the Brillouin-zone boundary (higher binding energies), the shorter this beating period becomes.

Figure 4 shows that the $n=1$ QWR is characterized by a good fit of the first large antinode of the envelope function into the Ag slab. When this happens, the electron becomes partially trapped in the slab, as indicated by a higher probability density. Likewise, the $n=2$ QWR is characterized by a good fit of the first two antinodes into the Ag slab. In between the two resonances, the wave function exhibits a reduced probability density within the Ag slab as evidenced by the curve for 0.9-eV binding energy.

Thus, QWR's are associated with enhanced probability densities within the Ag slab. This should lead to a higher photoemission intensity, because of the finite probing depth determined by the mean free path in the final state. A simple model for the photoemission intensity is thus to ignore any transition-matrix element effects, and to calculate the relative probability for the electron to be in the Ag slab:

$$I \propto \int_{z1}^{z0} |\psi_i|^2 dz,$$

where the limits of integration are the two boundaries of the slab. The results of this calculation are shown in Fig. 3. Clearly, the theoretical QWR peak positions and peak widths are well reproduced by this initial-state model calculation, although the relative intensities are off. Within this initial-state model, the peak positions are independent of the photon energy used to probe the initial wave-function localization,

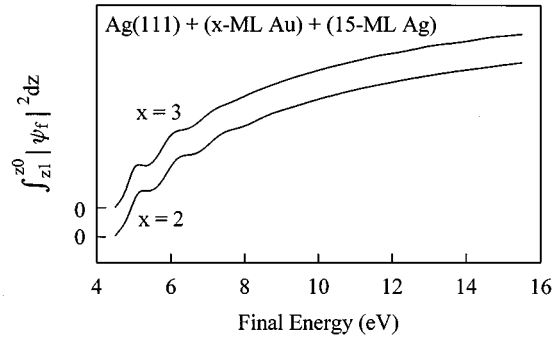


FIG. 5. The relative probability for the final state in the Ag slab as a function of the final energy, which is defined to be the electron energy above the Ag valence-band edge at 0.33 eV below the Fermi level. The two curves are offset vertically as indicated by the two zero marks on the vertical axis.

which is consistent with our experimental observation. Part of the discrepancy in the relative intensities is due to the density of states, but mostly, it is caused by a variation of the transition matrix element. The $n=3$ QWR as seen in Fig. 3 is enhanced by its proximity to the direct-transition peak. Near the direct transition, the short period oscillations in the initial and final states become better matched, leading to a coherent addition of intensity beyond what one might expect based on the envelope function alone.

When $n$ becomes large, more antinodes in the envelope function are cramped into the Ag slab (see Fig. 4). If the Ag slab has imperfections such as atomic steps or layer thickness fluctuations, the scattering caused by the imperfections will be proportional to the thickness scale of the imperfections divided by the wavelength of the envelope function. Thus, imperfections of the Ag slab structure at either the surface or the interface will cause a stronger damping for QWR's with large $n$'s. In the limiting case where the wavelength of the envelope function becomes the same as the layer thickness fluctuation, the $n$ and $(n+1)$ QWR's will become indistinguishable, and the peaks will simply merge. Although we do not have a quantitative measure of the film uniformity, it is conceivable that atomic steps and incomplete layering during sample growth can easily lead to an effective layer thickness fluctuation of $\pm 1$ ML. For the $n=3$ QWR, this would give rise to a perturbation on the order of $(2/15)\times n = 40\%$, and the binding energy of the QWR peak can become broadened by the same order, or $\sim$1 eV. A 1-eV broadening would make the $n=3$ peak nearly unrecognizable as seen in Fig. 3.

### D. Final wave functions

It is natural to wonder if the final-state wave functions will show a similar trapping behavior. Figure 5 shows the calculated relative probability within the Ag slab for the final state as a function of the final-state energy above the Ag valence-band edge for the two sample configurations. This probability approaches zero near the threshold for band-to-band transitions, as expected. Resonance features are observed at about 5 and 6 eV. These correspond to $n=2$ and 3 resonances, using the same numbering scheme as used above (the number of antinodes in the envelope function in the Ag

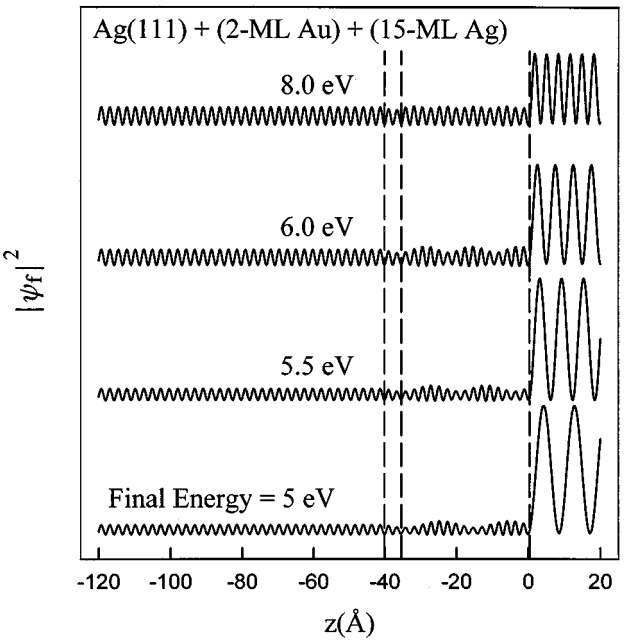


FIG. 6. The absolute square of the final wave function at several final energies above the Ag valence-band edge as indicated. The origin of the $z$ axis is at the classical surface plane. The vertical dashed lines indicate the various boundaries between Ag, Au, and vacuum for the sample with $x=2$.

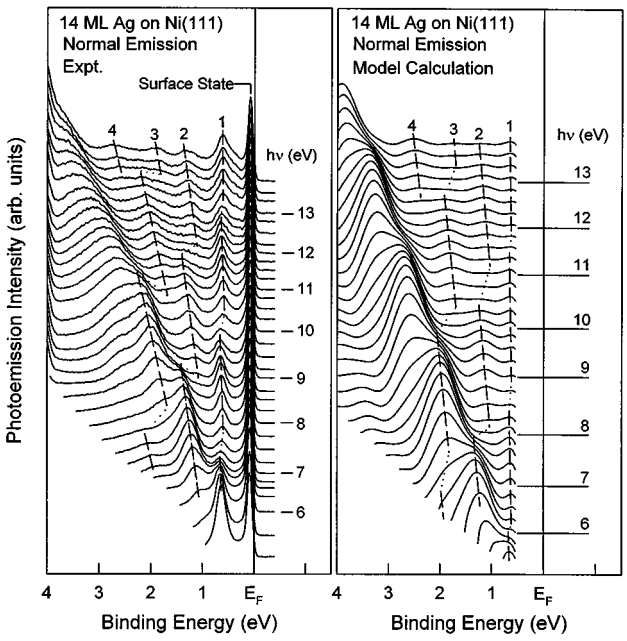


FIG. 7. Experimental (left) and theoretical (right) normal-emission spectra for 14 ML of Ag on Ni(111). The photon energies are indicated; the unlabeled spectra are taken at 0.25-eV intervals. The binding energy is referred to the Fermi level. The dashed curves indicate the peak movement, and the quantum numbers $n=1-4$ are indicated.

slab). The time-reversed LEED wave functions at these and two other energies are shown in Fig. 6. These resonances in the final state are rather subtle, and become very much damped at higher final energies. This is expected, since the effect of the interface potential should become less important as the electron energy increases. From a perturbation theory standpoint, it is the ratio between the interface potential and the electron energy that determines the strength of the perturbation. Using the same argument, it is easy to see that the initial-state resonance effects should be more important than the final-state resonance effects.

### E. Effects of lattice match/mismatch

A previous study of a Ag slab on Ni(111) shows intense QWR's that exhibit rather interesting behaviors.[17] The peaks move in a ratcheting fashion as the excitation photon energy is varied, and the intensities oscillate. For easy comparison, the experimental and theoretical spectra are reproduced here in Fig. 7. The behaviors are clearly of a different paradigm.

The main cause for this difference is the lattice mismatch for Ag on Ni. To explain this, consider the LEED state obtained by time reversing the photoemission final state. The incident electron partially penetrates the Ag slab to enter the Ni substrate. Due to the lattice mismatch, this beam is diffracted into many different beams corresponding to various linear combinations of the surface reciprocal-lattice vectors of Ag and Ni (diffraction by a Moire grating). As a result, many beams emerge, traveling in all sorts of directions. The initial state is affected by a similar effect. Dipole transitions for states within the Ni substrate that are traveling in different directions are generally forbidden, and so the dipole matrix element as a whole for the Ni substrate becomes very much reduced. In our Ag/Ni calculation, we simply ignored this portion of the matrix element. The truncation of the matrix element integral at the Ag/Ni interface effectively broadens the electron wave vector and causes side bands to form just as a single slit diffraction pattern in optics. As the photon energy is varied, the broadened initial- and final-state resonances move in and out of the energy window of the experiment, causing the appearance of ratcheting peaks.

For Ag/Au/Ag, the states are ''anchored'' by the substrate to have well-defined wave vectors, resulting in QWR's with fixed binding energies. It is possible that some systems may show behaviors somewhere in between the Ag/Au/Ag and Ni/Ag cases. One possibility is a lattice mismatched system with a simple lattice-constant ratio, for which a simple superstructure can form; this can result in a reduced but nonzero Moire diffraction effect.

## VI. SUMMARY AND CONCLUSIONS

Using Ag/Au/Ag as a model barrier system, we have investigated various aspects of the electronic properties of a leaky quantum well, and the photoemission features that are associated with these properties. We have observed well-defined QWR's for Au barriers as thin as 2 ML. These QWR's can be well described by an initial-state model, in which wave function trapping in the Ag slab accounts for the resonance features. The QWR peaks do not disperse as the excitation photon energy is varied, in sharp contrast to a previously studied system, Ag on Ni(111). The difference is attributed to the lattice mismatch between Ag and Ni. Final-state effects are important for Ag/Au/Ag near the direct transitions. The theoretical model employed in this study in-

volves the band structure and surface properties, and the results are generally in good agreement with the data, except for the extra broadening of the QWR's. We believe that this extra broadening, which depends on the quantum number $n$, is a result of imperfections of the film such as the presence of atomic steps and layer thickness fluctuations. We are in the process of extending the systematics developed in this study to magnetic systems, in which spin polarization, $d$-band mixing, and lattice mismatch will add some degrees of complexity to the experiment and the analysis. The present work will serve as a useful basis for such a study. Our goal is to describe the electronic and magnetic properties of such systems in terms of basic quantities such as the wave function and band structure.

**ACKNOWLEDGMENTS**

This material is based upon work supported by the U.S. National Science Foundation, under Grant No. DMR-92-23546. Acknowledgment is also made to the Donors of the Petroleum Research Fund, administered by the American Chemical Society, and to the U.S. Department of Energy, Division of Materials Sciences, (Grant No. DEFG02-91ER45439) for partial support of the synchrotron beamline operation and for support of the central facilities of the Materials Research Laboratory. The Synchrotron Radiation Center of the University of Wisconsin is supported by the National Science Foundation under Contract No. DMR-95-31009.

*Present address: National Renewable Energy Laboratory, Golden, Colorado 80401.

[1] R. C. Jaklevic and J. Lambe, Phys. Rev. B **12**, 4146 (1975).

[2] B. T. Jonker, N. C. Bartelt, and R. L. Park, Surf. Sci. **127**, 183 (1983).

[3] M. Jalochowski and E. Bauer, Phys. Rev. B **38**, 5272 (1988).

[4] P. D. Loly and J. B. Pendry, J. Phys. C **16**, 423 (1983).

[5] T. Miller, A. Samsavar, G. E. Franklin, and T.-C. Chiang, Phys. Rev. Lett. **61**, 1404 (1988).

[6] S. Å. Lindgren and L. Wallden, Phys. Rev. Lett. **61**, 2894 (1988).

[7] J. E. Ortega, F. J. Himpsel, G. J. Mankey, and R. F. Willis, Phys. Rev. B **47**, 1540 (1993); J. E. Ortega and F. J. Himpsel, Phys. Rev. Lett. **69**, 844 (1992).

[8] D. A. Evans, M. Alonso, R. Cimino, and K. Horn, Phys. Rev. Lett. **70**, 3483 (1993).

[9] F. Patthey and W.-D. Schneider, Phys. Rev. B **50**, 17 560 (1994).

[10] J. L. Prinz, Phys. Today **48** (4), 24 (1995).

[11] K. Derbyshire and E. Korczynski, Solid State Technol. **38** (9), 57 (1995).

[12] J. L. Simonds, Phys. Today **48** (4), 26 (1995).

[13] L. M. Falicov, Phys. Today **45** (10), 46 (1992).

[14] A. C. Ehrlich, Phys. Rev. Lett. **71**, 2300 (1993).

[15] J. M. Gallego, D. Lederman, S. Kim, and I. K. Schuller, Phys. Rev. Lett. **74**, 4515 (1995).

[16] See, for example, M. van Schilfgaarde and W. A. Harrison, Phys. Rev. Lett. **71**, 3870 (1993); B. A. Jones and C. B. Hanna, *ibid.* **71**, 4253 (1993); M. C. Munoz and J. L. Perez-Diaz, *ibid*. **72**, 2482 (1994).

[17] T. Miller, A. Samsavar, and T.-C. Chiang, Phys. Rev. B **50**, 17 686 (1994).

[18] R. J. Culbertson, L. C. Feldman, P. J. Silverman, and H. Boehm, Phys. Rev. Lett. **47**, 675 (1981); T. C. Hsieh, T. Miller, and T.-C. Chiang, Phys. Rev. B **33**, 2865 (1986). In the latter study, a Au monolayer buried in Ag showed an exponential attenuation of the Au core-level emission intensity as a function of the depth of the Au layer below the sample surface.

[19] P. S. Werner, R. S. Williams, S. D. Kevan, D. Denley, and D. A. Shirley, Phys. Rev. B **19**, 6164 (1979).

[20] J. G. Nelson, S. Kim, W. J. Gignac, R. S. Williams, J. G. Tobin, S. W. Robey, and D. A. Shirley, Phys. Rev. B **32**, 3465 (1985).

[21] R. Paniago, R. Matzdorf, G. Meister, and A. Goldmann, Surf. Sci. **336**, 113 (1995), and references therein.

[22] N. V. Smith, Phys. Rev. B **32**, 3549 (1985), and references therein.

[23] W. E. McMahon, T. Miller, and T.-C. Chiang, Mod. Phys. Lett. B **8**, 1075 (1994).

[24] G. D. Mahan, Phys. Rev. Lett. **24**, 1068 (1970); Phys. Rev. B **2**, 4334 (1970).

[25] The mean free path used here is derived from an analysis of the direct-transition line shape for pure Ag(111). The width of this peak is mostly determined by the mean free path and the group velocities of the initial and final states. The initial-state broadening plays a relatively minor role. The relevant formula can be found in T.-C. Chiang, J. A. Knapp, M. Aono, and D. E. Eastman, Phys. Rev. B **21**, 3513 (1980) and in J. B. Pendry, in *Photoemission and the Electronic Properties of Surfaces*, edited by B. Feuerbacher, B. Fitton, and R. F. Willis (Wiley, New York, 1978), pp. 87–109.

[26] A very common approximation for photoemission calculation is the three-step model, in which the photoexcitation in the sample, transport to the surface (inelastic scattering), and escape to the vacuum are assumed to be incoherent, independent steps. See, N. W. Ashcroft, in *Photoemission and the Electronic Properties of Surfaces* (Ref. 25), pp. 21–44.